FIRST OPERATION OF A ROTATING TEST RIG FOR TRANSIENT THERMOCHROMIC LIQUID CRYSTAL HEAT TRANSFER EXPERIMENTS

C. Waidmann, R. Poser, M. Göhring, J. von Wolfersdorf

Institute of Aerospace Thermodynamics (ITLR),
University of Stuttgart,
Germany

Keywords: heat transfer, turbine blade, internal cooling, transient thermochromic liquid crystal

ABSTRACT

A test rig for the investigation of rotating turbine blade internal cooling channel configurations is presented. The heat transfer is measured using the transient thermochromic liquid crystal (TLC) technique. The rig can be operated at rotational speeds of up to 900 rpm, mass flow rates between 5 g/s and 30 g/s, a fluid temperature between -100°C and +80°C and a pressure of up to 10 bar. This allows for a broad range of possible test conditions. The investigated cooling channel model is a two-pass leading edge configuration. It consists of a first pass with a trapezoidal cross-section and radial outward flow, a 180-degree bend, and a second pass with a rectangular cross-section and radial inward flow. The suction side and pressure side surfaces are ribbed.

The transient evaluation method is based on the measurement of TLC indication times. A fluid temperature change is applied to induce a color play on the TLC-coated heat transfer surfaces. This color play is captured using cameras that are rotating with the test model. A remote controlled camera unit with integrated batteries, LED lighting and a signal-LED for synchronization purposes has been developed and is presented in this paper.

In order to reproduce the correct sense of the buoyancy forces, the heat flux needs to be in the correct direction, i.e. from a warm channel wall to a colder cooling fluid. Therefore, liquid nitrogen cooled air is used as cooling fluid with the test model at ambient temperature. Precooling of the air supply pipes inside the rotor prevents the test air to heat up excessively before reaching the test model. This is essential especially for low mass flow rates. A radio telemetry system collects temperature and pressure data from inside the rotating model housing and allows real time monitoring.

NOMENCLATURE

η	Dynamic viscosity
ρ	Density of fluid
λ_f	Thermal conductivity of fluid
Ω	Rotational speed [rad/s]
A	Cross-section area of channel
Bo	Buoyancy number
d_h	Hydraulic diameter
h	Heat transfer coefficient
$\dot{m}$	Mass flow rate
n	Rotational speed [rpm]
Nu	Nusselt number
PS	Pressure side
$PROTEIN$	In-house code for heat transfer evaluation
R	Mean model radius
Re	Reynolds number
Ro	Rotation number
s	Stream wise distance
SS	Suction side
t	Time
T_f	Fluid temperature
T_w	Wall temperature
TLC	Thermochromic liquid crystal
u	Fluid velocity

INTRODUCTION

In an effort to increase the overall efficiency of turbojet engines, the turbine blade cooling air consumption of modern engines is being constantly reduced. However, with decreasing cooling air mass flow rates, the influence of rotation on the flow and thus the heat transfer distribution inside rotating cooling channels increases. Future cooling system designs will be more and more dependent on the understanding of these rotational effects.

As described in Waidmann et al. (2016) several test approaches and test rig designs have been developed and applied to investigate rotational effects on heat transfer in the 1990ies, e.g. Wagner et al. (1991), Morris (1996), Blair et al. (1991) and Davenport (1998). Blair et al. and Davenport thereby applied the transient TLC measurement technique, which is also applied in more recent developments, e.g. Pagnacco et al. (2016), Mathison et al. (2017) as well as considered here.

EXPERIMENTAL SETUP

The design of the rig is presented by Waidmann et al. (2016). The rotor consists mainly of a hollow main shaft, hollow rotor arm, model housing and an adjustable counterweight on the

opposing counterweight arm. An overview of the rig is given in Figure 1.
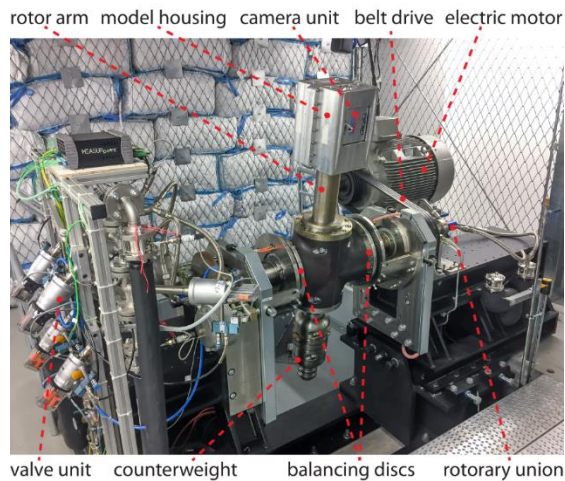
Figure 1: Test rig overview

The test model is positioned inside a model housing which consists of two aluminum half shells and can be operated with air pressures of up to 10 bar. The housing is mounted at the end of the rotor arm so that the model is positioned at a mean model radius of 750 mm.

An electric motor with frequency converter drives the rotor up to a maximum rotational speed of 900 rpm via a belt drive. Vibration velocity sensors on both bearing housings are used by a balancing system to calculate the masses and positions of balancing weights. These weights are mounted to the main counterweight for balancing in one plane and to the balancing discs on both sides of the rotor for fine balancing in two planes.

Test air supply is controlled by a valve unit containing six fast switching valves. The unit allows to switch between two separate air flows. The tempering air flow keeps the test model isothermal at ambient temperature and pressurizes the model before the experiment. The experiment starts by switching from the tempering air flow to the cold test air flow which induces the fluid temperature change needed for the transient TLC experiment.

ROTOR

Both shaft ends of the rotor are equipped with rotary unions by *Deublin* to introduce air into the rotating system. Figure 2 shows the air passages inside the rotor. The rotary union on the left is directly connected to the model and provides the tempering air (before the experiment) and the test air (during the experiment). The rotary union on the right-hand side feeds a separate secondary pipe system with precool air which is used to cool down the test air supply pipes prior to the experiment. For this purpose, the air supply pipes consist of three integrated pipes. The central pipe leads the test air to the model. The outer pipes contain the

precool air. Precooling of the air supply pipes prevents the test air to heat up excessively before reaching the test model and guarantees a suitable fluid temperature change for the transient TLC experiment.
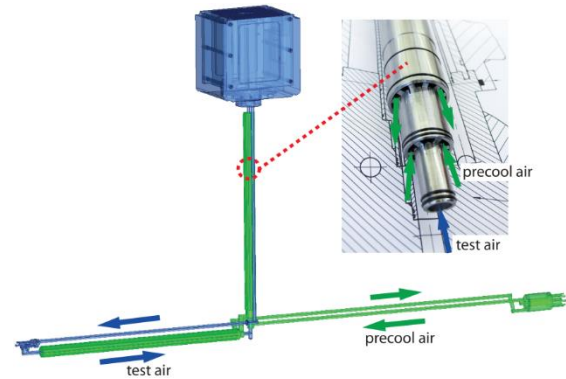
Figure 2: Air passages inside the rotor

TEST MODEL

The cooling channel geometry is derived from a model that was investigated on a non-rotating test rig by Waidmann et al. (2013). Figure 3 shows the CAD-representation of the fluid domain as well as the orientation of the channel cross-section with respect to the rotational axis.
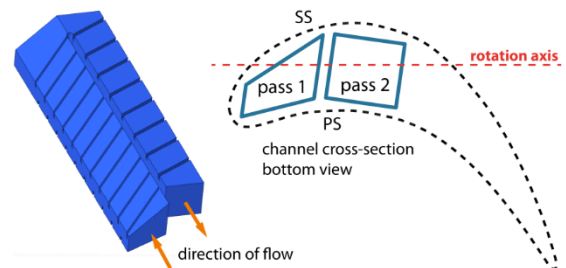
Figure 3: Cooling channel geometry

The inlet passage (pass 1) has a trapezoidal cross-section and represents a leading edge cooling channel with a radial outward flow. The hydraulic diameter is d_{h1}=15 mm. A 180° bend connects pass 1 with the outlet passage (pass 2) with a rectangular cross-section and radial inward flow. The hydraulic diameter of pass 2 is d_{h2}=19.89 mm.

The suction side (SS) and pressure side (PS) surfaces are ribbed in a staggered fashion with rib angles of 60° to 65°. The test model consists of two Perspex half-shells that are mounted inside an aluminum frame, see Figure 4.

The inner channel walls are coated with TLCs and black backing paint. Narrowband TLCs (type SPN100/G0C1W) with an indication temperature of 0 °C and a bandwidth of 1 K by *Hallcrest* are used. The model is instrumented with three thermocouples type K in the flow at the inlet, bend and outlet. The thermocouples are wedged between

4

the two half-shells with the tip directed to the geometric center of the respective cross-section.
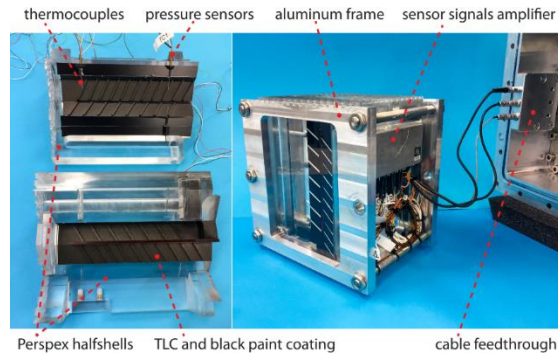
Figure 4: Test model

Absolute pressure sensors by *Kulite* are positioned at the inlet and outlet. All sensors are connected to a sensor signal amplifier which is directly mounted to the side of the model, see Figure 4. The sensor signal amplifier is part of a customized radio telemetry system by *Manner* and provides 22 temperature and 6 pressure channels.

To monitor the temperature distribution inside the model, additional 10 thermocouples are mounted at different depth inside the Perspex block. Five thermocouples are positioned near the inlet region and five near the bend region of the first passage. The distances of the thermocouple tips perpendicular to the channel wall are 3 mm, 6 mm, 9 mm, 12 mm and 15 mm. With this instrumentation it is possible to check, if the model is isothermal before the start of the experiment. Also the temperature profile development inside the Perspex during the experiment can be measured. Thus, the validity of the semi-infinite wall assumption of the heat transfer evaluation can be assessed.

ROTATING CAMERA UNIT

A camera unit was designed to be mounted inside the model housing in order to capture the TLC color play during rotation, see Figure 5 .

The unit consists of a customized *Mobius* action camera, lighting and signal LEDs, IR receiver and batteries integrated in an aluminum plate. The camera has a 1080p Full HD resolution at a framerate of 30 fps. Two units are used to capture the suction side and pressure side simultaneously. The 145° wide angle lens allows a camera position very near to the model. Camera lens and sensor are encapsulated and covered by protective glass. This way any possible deformations and thereby video distortions due to operating pressures of up to 10 bar are prevented.

Four white *Luxeon Rebel* LEDs with a color temperature of 6500 K and a maximum luminous flux of 180 Lumen are positioned in the corners of

the unit providing a homogeneous illumination of the model.
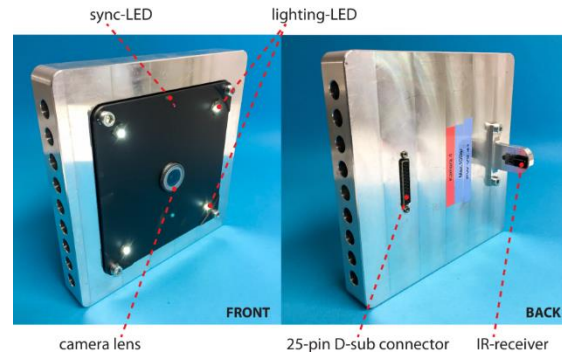
Figure 5: Camera unit

A single red LED is used for synchronization of the video with the fluid temperature measurements. The reflection of the LED on the Perspex model is visible in the video while the switching of the LED is timed with external data acquisition.

Camera and LEDs are activated via a coded IR remote control. The IR receiver is positioned on a small cantilever mounted on the back of the unit. This ensures an unobstructed line of sight between IR sender and receiver independent from the orientation of the model housing or position of the rotor arm.

The unit is powered by four LiFePo4 batteries with a total capacity of 9600 mAh. A 25-pin D-sub connector provides the USB interface for the configuration of the camera settings and downloading the videos from the internal micro SD memory card. Recharging of the batteries is also done via this connector. The front side is coated matt black to reduce reflections in the Perspex model.

FLUID TEMPERATURE CHANGE

The fluid temperature change is generated with the help of a bypass valve unit which controls the air supply to the model. In the *tempering state* the tempering air is lead through the rotor passage. This air flow is either at ambient temperature or slightly heated and fulfills three functions. First, it defines the isothermal starting temperature for the Perspex model. Second, it prevents cold air from the precooled central pipes of the rotor arm and the shaft to enter the model before the experiment. For this purpose, the flow direction is reversed compared to the flow direction during the experiment, see Figure 6. And third, it sets a suitable pressure level to prevent a pressure jump at the start of the experiment, when the cold test air is switched to the rotor passage (*experiment state*). The precool air and test air can be cooled down to temperatures as low as -100°C with the help of a

heat exchanger that is operated with liquid nitrogen.
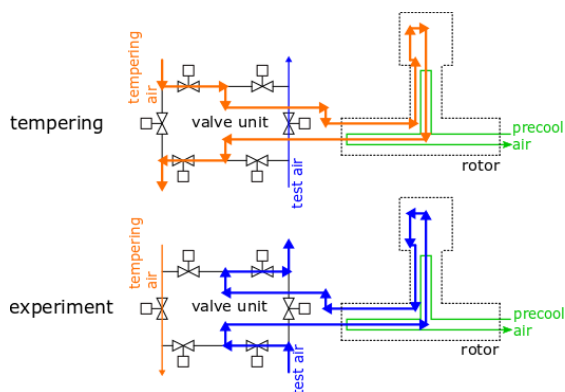
Figure 6: Valve unit setting for tempering state and experiment state

Figure 7 shows a typical fluid temperature change for an experiment with a mass flow rate of ṁ=10 g/s (Re≈31500 at d_h=15 mm). At the model inlet the fluid temperature drops rapidly below the TLC indication temperature. As the test air heats up on its way through the channel, the temperature change at the bend and at the outlet are delayed accordingly.
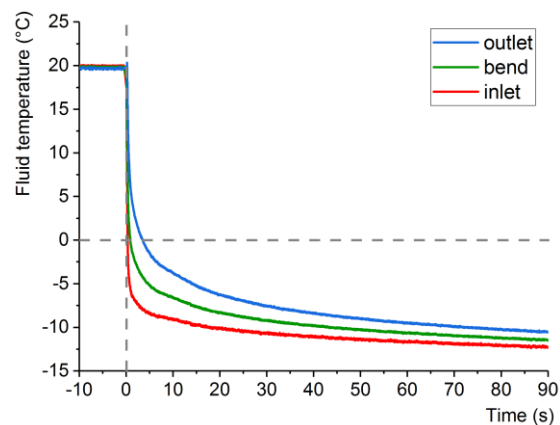
Figure 7: Fluid temperature change

The corresponding temperature change at different depths inside the Perspex wall is given in Figure 8. During the duration of the test (approx. 90 s), the temperature at a depth of 3 mm decreases by approx. 10 K, while the temperature at 15 mm remains virtually unchanged. The Perspex model was designed with a minimum wall thickness of 20 mm. Hence, for this experimental setting, the assumption of a semi-infinite wall is fulfilled, as required by the evaluation method.

DATA ACQUISITION

The measurement data acquisition is based on a PXI-System by *National Instruments.* A NI-PXI-6602 Counter/Timer module is used to generate a synchronization signal marking the start of the experiment. Simultaneously an IR-signal is sent to the camera unit to switch off the sync-LED in order to get a temporal reference point in the video footage.
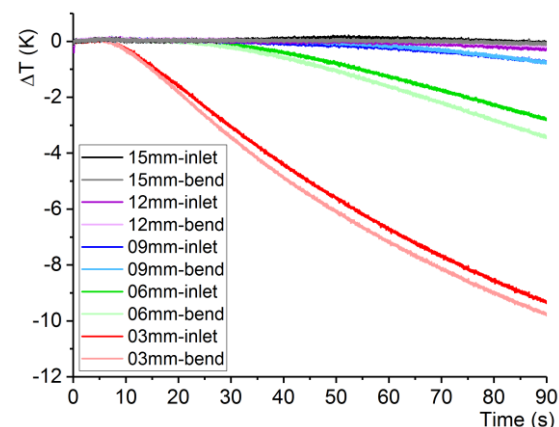
Figure 8: Perspex temperature change

The PXI-System then generates the control signals for the valve unit to switch from the *tempering state* to the *experiment state*. The six valves can be preprogrammed with individual delay times providing the possibility to optimize the switching procedure with regard to pressure and mass flow rate.

The telemetry system broadcasts the temperature and pressure data form the model as digitized 16-bit signals. At the receiver unit these signals are converted to analog voltage signals with a range of -10 V to +10 V. These voltages are then measured with a NI-PXIe-6345 multifunction I/O module. This module is also used to log the valve positions, which are equipped with inductive sensors for both the open and the closed position. An additional NI-PXI-6238 multifunction I/O module acquires the current signals of six PXM319-015AI pressure transducers by *Omega* which are mounted to key positions at the valve unit. All PXI modules are connected by a dedicated synchronization bus and are configured to use the same time base and a constant sample rate of 100 samples/s.

The mass flow rate of the test air is measured by a Promass 83F15 Coriolis flowmeter by *Endress + Hauser.* The rotational speed is provided by a custom-designed rotary encoder consisting of a disk with 15 evenly distributed radial boreholes, an inductive sensor BES040R by *Balluff* and a counter module 6ES7138 by *Siemens.* Mass flow rate and rotational speed are logged at a rate of 10 samples/s.

DATA PROCESSING AND ANALYSIS

The transient TLC technique is based on the measurement of TLC indication times following an induced fluid temperature change. A detailed description of this technique is presented by Ireland and Jones (2000) and Poser et al. (2005, 2007).

Prior to evaluation of the video footage with the in-house code PROTEIN, a few post processing steps have to be performed. Using the sync-LED information, the video is cut, so that the start of the video is synchronized with the start of the fluid temperature drop registered at the inlet thermocouple. Then the fisheye distortion caused by the wide angle lens is corrected using the B-spline based dewarp algorithm bUnwarpJ developed by Arganda-Carreras et al. (2006). This algorithm is included as a plugin in the open source image processing software Fiji by Schindelin et al. (2012). After that, the video is cropped to the relevant heat transfer surface.

The first analysis steps in PROTEIN are wavelet based filtering and adaptive normalization as described by Poser et al. (2009). An exemplary frame of the original video of the pressure side and the corresponding frame of the processed, filtered, and normalized video are given in Figure 9 and Figure 10.
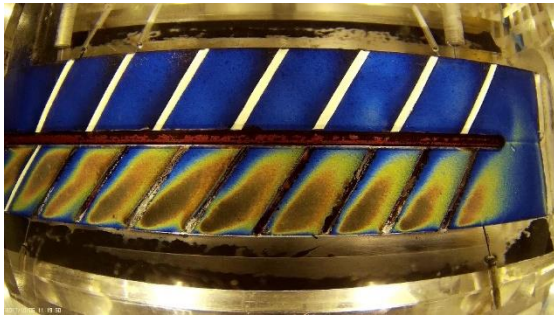
Figure 9: Frame of original video (pressure side)
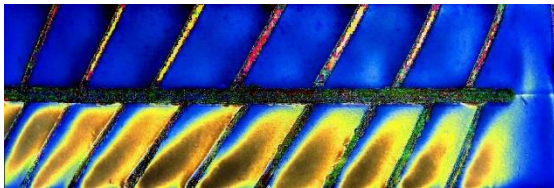
Figure 10: Frame of processed video (pressure side)

PROTEIN then evaluates for each pixel the time at which the intensity of the green channel reaches its maximum, i.e. the time at which the surface reaches the TLC indication temperature. This temperature is determined beforehand in a stationary calibration process as described by Poser et al. (2010). Using the thermocouple data, the fluid temperature history is calculated for each pixel. Thereof, together with the corresponding indication times the heat transfer coefficients as well as the Nusselt numbers can be determined for every pixel.

DIMENSIONLESS QUANTITIES

The Reynolds number is calculated from the mass flow rate, the channel geometry, and the dynamic viscosity, which is derived from the temperature at the channel inlet.

$$Re = \frac{\rho\, u\, d_h}{\eta} = \frac{\dot{m}\, d_h}{A\, \eta} \qquad (1)$$

The Rotation number is calculated from the rotational speed, hydraulic diameter, and the flow velocity, which is derived from the pressure and temperature at the channel inlet.

$$Ro = \frac{\Omega\, d_h}{u} \qquad (2)$$

The Buoyancy number is calculated from the temperature difference between channel wall and fluid, the Rotation number, and the ratio between model radius and hydraulic diameter. For the wall temperature T_w the isothermal start temperature of the model is chosen. The fluid temperature T_f is determined at the channel inlet.

$$Bo = \frac{\Delta\rho}{\rho} Ro^2 \frac{R}{d_h} = \left(\frac{T_w - T_f}{T_w}\right) Ro^2 \frac{R}{d_h} \qquad (3)$$

Figure 11 shows the exemplary development of the Reynolds number, Rotation number, and Bouyancy number for an experiment with a mass flow rate of ṁ=10 g/s. Here, the dimensionless quantities are normalized with their respective nominal values for this experiment, namely Re_nom=31500, Ro_nom=0.144 and Bo_nom=0.11.
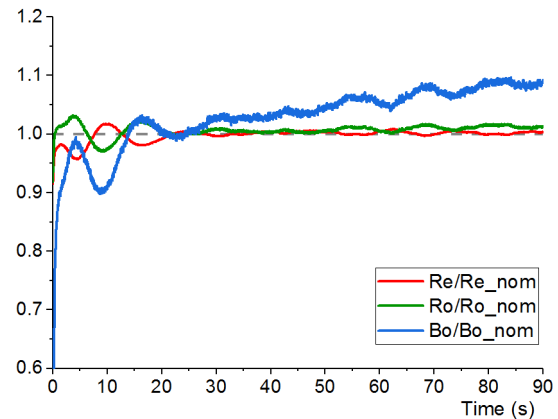
Figure 11: Development of normalized dimensionless quantities Re, Ro, and Bo

The fluctuations of these dimensionless quantities at the start of the experiment are caused by the mass flow control, which needs to compensate for the increased pressure drop after the test air is switched from bypass into the rotor passage. After the fluctuations subside, the Reynolds number and Rotation number approximate a constant value, respectively. The Buoyancy number, however, is steadily increasing, as the fluid temperature at the inlet is steadily decreasing, as shown in Figure 7.

The Nusselt number is calculated from the heat transfer coefficient, the hydraulic diameter, and the thermal conductivity of the fluid. The latter is an

averaged value considering the local fluid temperature history between the start of the experiment and the respective TLC indication time.

$$Nu = \frac{h\,d_h}{\lambda_f} \qquad (4)$$

RESULTS

In this section some exemplary results of a rotating and a non-rotating experiment are presented. Between the experiments only the rotational speed has been varied (0 rpm and 400 rpm). The flow conditions, i.e. mass flow rate, temperature, and pressure settings have not been altered to obtain comparable Reynolds numbers. Figure 12 and Figure 13 show the resulting Nusselt number distributions for both experiments.
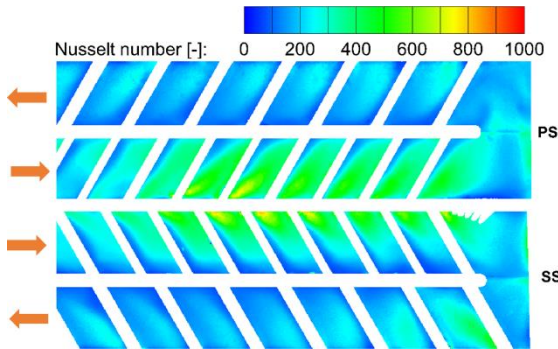
Figure 12: Nusselt number distribution of non-rotating experiment (n=0 rpm / Re=31500 / Ro=0 / Bo=0)
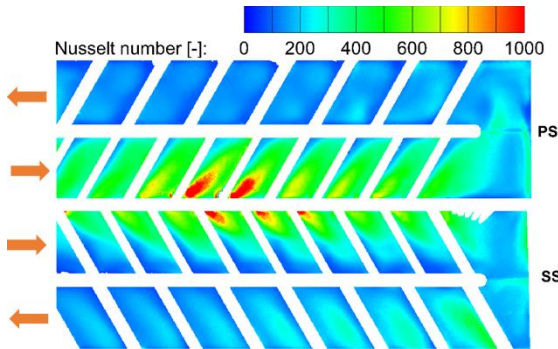
Figure 13: Nusselt number distribution of rotating experiment (n=400 rpm / Re=31500 / Ro=0.144 / Bo=0.11)

A means to show the direct influence of rotation on the heat transfer distribution is the calculation of local Nusselt number ratios, as shown in Figure 14. It can be seen, that rotational effects can locally increase the heat transfer by a factor of two and more (e.g. pass 1 of PS). However, depending on the flow direction and orientation of the surface with respect to the rotational axis, the heat transfer can also be substantially decreased (e.g. pass 2 of PS).

Any possible systematic measurement errors should affect the obtained absolute Nusselt number values for both experiments in the same direction. By forming Nusselt number ratios, the influence of systematic measurement errors can be minimized.
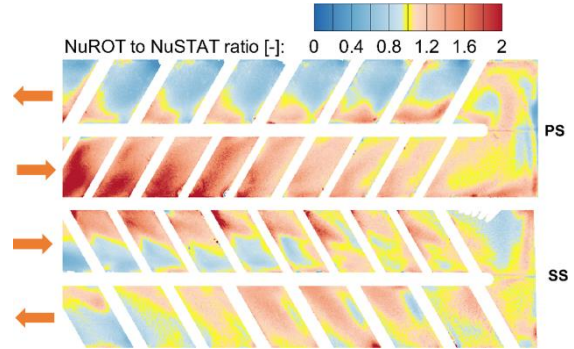
Figure 14: Local Nusselt number ratios (NuROT to NuSTAT)

A data reduction method is shown in Figure 15. In the contour plots of the Nusselt number distribution, averaging lines parallel to the ribs are chosen, as depicted by the red dashed lines. The resulting averaged values are then plotted against the normalized stream wise distance s. The zero-point of s is specified at the channel top wall, so that negative values refer to pass 1 and positive values to pass 2.
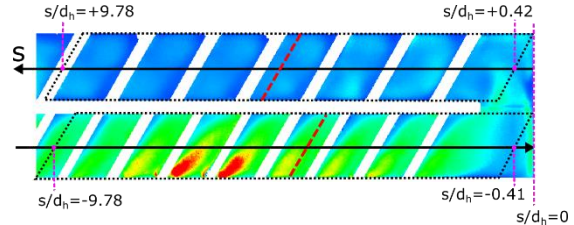
Figure 15: Description of averaging lines (red dashed lines) and definition of stream wise distance s

Figure 16 and Figure 17 show the results of the data reduction for both experiments.
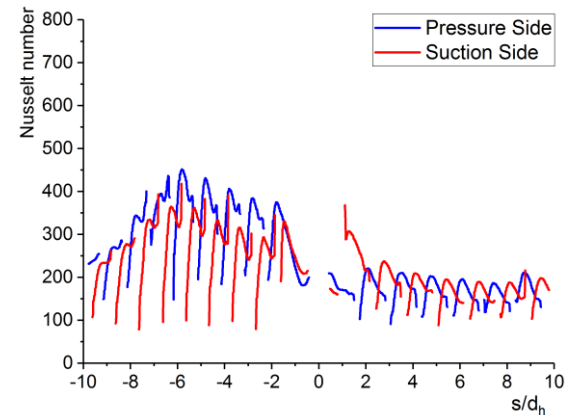
Figure 16: Line averaged Nusselt numbers of non-rotating experiment (n=0 rpm / Re=31500 / Ro=0 / Bo=0)
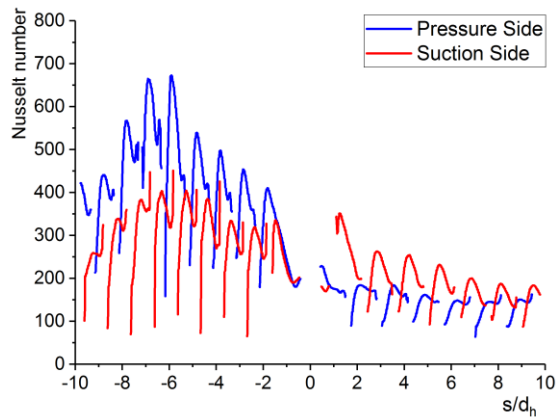
Figure 17: Line averaged Nusselt numbers of rotating experiment (n=400 rpm / Re=31500 / Ro=0.144 / Bo=0.11)

Figure 18 shows the NuROT to NuSTAT ratio of the line averaged Nusselt numbers.
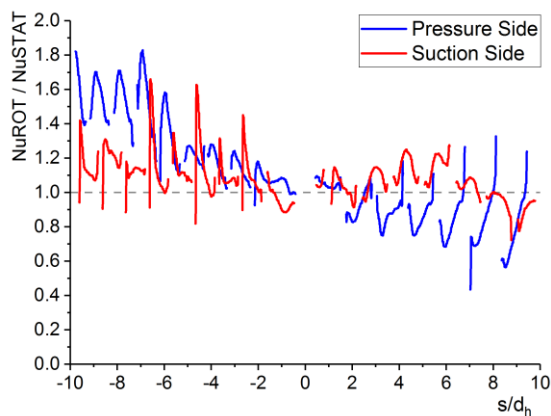
Figure 18: Line averaged Nusselt number ratios (NuROT to NuSTAT)

CONCLUSION

A rotating test rig for heat transfer experiments using the transient TLC technique has been presented. Newly developed co-rotating camera units are employed to capture the TLC color play. The process of generating the required fluid temperature change with the help of a bypass valve unit has been described. For a typical experiment, the fluid temperature history as well as the temperature history at different depths inside the Perspex wall have been depicted. Finally, a comparison between a typical rotating and the corresponding non-rotating experiment have been presented. The results have been outlined as Nusselt number distributions as well as line averaged values. Furthermore, Nusselt number ratios (rotating to stationary) have been presented for a direct assessment of rotational effects on the heat transfer distribution.

ACKNOWLEDGEMENTS

REFERENCES

[1] Arganda-Carreras, I.; Sorzano, C. O. S.; Marabini, R.; Carazo, J. M.; de Solorzano, C. O.; Kybic, J.; 2006. "Consistent and Elastic Registration of Histological Sections Using Vector-Spline Regularization". Lecture Notes in Computer Science, Springer Berlin / Heidelberg, volume 4241/2006, CVAMIA: Computer Vision Approaches to Medical Image Analysis, pp. 85-95, ISBN: 3-540-46257-0.

[2] Blair, M. F.; Wagner, J. H.; Steuber, G. D.; 1991. "New applications of liquid crystal thermography in rotating turbomachinery heat transfer research". ASME, International Gas Turbine and Aeroengine Congress and Exposition, 36th, Orlando, FL, June 3-6, 1991. 11 p.

[3] Davenport, R.; 1998. "The Benefits of a Rotating Rig for Research into Advanced Turbine Cooling Systems". RTO MEETING PROCEEDINGS 8. RTO Applied Vehicle Technology Panel (AVT) Symposium, Toulouse, France.

[4] Ireland, P. T.; Jones, T. V.; 2000. "Liquid crystal measurements of heat transfer and surface shear stress". Measurement Science and Technology 11 (7), pp. 969–986. DOI: 10.1088/0957-0233/11/7/313.

[5] Mathison, R. M.; Dunn, M. G.; 2017. "A New Rotating Facility for Investigating Cooling Passage Internal Heat Transfer". Proceedings of the 1st Power and Propulsion Forum. GPPF-2017-158.

[6] Morris, W. D.; 1996. "A rotating facility to study heat transfer in the cooling passages of turbine rotor blades". Proceedings of the Institution of Mechanical Engineers, Part A: Journal of Power and Energy 1990-1996 (vols 204-210) 210 (11), pp. 55–63.

[7] Pagnacco, F.; Furlani, L.; Armellini, A.; Casarsa, L.; Davis, A.; 2016. "Rotating Heat Transfer Measurements on a Multi-Pass Internal Cooling Channel: I - Rig Development". ASME. Turbo Expo, Volume 5B: Heat Transfer: V05BT16A005. DOI:10.1115/GT2016-56308.

[8] Poser, R.; Ferguson, J. R.; von Wolfersdorf, J.; 2009. "Temporal Signal Preprocessing and Evaluation of Thermochromic Liquid Crystal Indications in Transient Heat Transfer Experiments". 8th European Conference on Turbomachinery Fluid Dynamics and Thermodynamics, pp. 785–795.

[9] Poser, R.; von Wolfersdorf, J.; 2010. "Transient liquid crystal thermography in complex internal cooling systems". VKI Lecture Series - Internal Cooling in Turbomachinery, von Karman Institute for Fluid Dynamics (VKI LS 2010-05).

[10] Poser, R.; von Wolfersdorf, J.; Lutum, E.; 2007. "Advanced evaluation of transient heat transfer experiments using thermochromic liquid crystals". Proceedings of the Institution of Mechanical Engineers, Part A: Journal of Power and Energy 221 (6), pp. 793–801.

[11] Poser, R.; von Wolfersdorf, J.; Semmler, K.; 2005. "Transient Heat Transfer Experiments in Complex Passages". Proceedings of HT2005 ASME Summer Heat Transfer Conference, HT2005-72260. July 17-22, 2005, San Francisco, California, USA.

[12] Schindelin, J.; Arganda-Carreras, I.; Frise, E.; Kaynig, V.; Longair, M.; Pietzsch, T. et al.; 2012. "Fiji: an open-source platform for biological-image analysis". Nat Methods 9 (7), pp. 676–682. DOI: 10.1038/nmeth.2019.

[13] Wagner, J. H.; Johnson, B. V.; Hajek, T. J.; 1991. "Heat Transfer in Rotating Passages with Smooth Walls and Radial Outward Flow". ASME J. of Turbomachinery, 113, pp. 42–51.

[14] Waidmann, C.; Poser, R.; Nieland, S.; von Wolfersdorf, J.; 2016. "Design of a Rotating Test Rig for Transient Thermochromic Liquid Crystal Heat Transfer Experiments". ISROMAC 2016, International Symposium on Transport Phenomena and Dynamics of Rotating Machinery, Hawaii, Honolulu, April 10-15, 2016.

[15] Waidmann, C.; Poser, R.; von Wolfersdorf, J.; Fois, M.; Semmler, K.; 2013. "Investigations of Heat Transfer and Pressure Loss in an Engine-Similar Two-Pass Internal Blade Cooling Configuration". 10th European Conference on Turbomachinery Fluid Dynamics and Thermodynamics, Lappeenranta, Finland, pp. 1051–1063.

http://www.euroturbo.eu/paper/ETC2013-168.pdf.